

Fully Integrated Wireless Elastic Wearable Systems for Health Monitoring Applications

Mohammad H. Behfar¹, Donato Di Vito², Arttu Korhonen³, Dung Nguyen⁴, Belal Mostafa Amin,
Timo Kurkela⁵, Markus Tuomikoski, and Matti Mäntysalo⁶, *Member, IEEE*

Abstract—Advances in flexible and hybrid electronics promote increasing demands for wearable sensors in personal health, monitoring, and diagnostic medical gadgets. Conventional wearable devices rely on electronics based on rigid substrates and components with limited conformity to user skin. In this work, we report a fully integrated, stretchable wireless electrocardiography (ECG) system developed on highly elastic, ultra-thin (100 μm) thermoplastic polyurethane (TPU) film without any rigid or flexible interposer. Moreover, the circuit layout printing and component assembly are carried out through sheet-to-sheet (S2S) process directly on TPU film. This study utilizes both experimental reliability tests coupled with data acquired from finite element modeling (FEM) to assess performance and failure of the device under tensile loading. In such a complex system assembly, FEM simulation not only provides insights on the overall electromechanical performance of the device, but also facilitates localization of the failure points which are difficult to access for visual inspection. The performance of the device is also evaluated through controlled uniaxial cyclic strain at 5% and 10% elongation. The durability test shows that the assembled device can stay functional over hundreds of deformation cycles, suggesting that direct assembly of conventional components on stretchable substrate represents a promising approach for fully integrated stretchable devices, which is a step toward scalable manufacture of wearable stretchable electronics through high-throughput manufacturing processes.

Index Terms—Printed stretchable electronics, skin patch, wearable sensors, wireless sensors.

I. INTRODUCTION

WEARABLE sensors receive increasing attention, as advances in integration of hybrid electronics can realize extremely conformal wearable skin patches on flexible

Manuscript received September 18, 2020; revised April 30, 2021; accepted May 11, 2021. Date of publication May 21, 2021; date of current version June 16, 2021. This work was supported in part by the Business Finland under Grant 3087/31/2018 and Grant 2947/31/2018 and in part by the Academy of Finland [utilized the Printed Intelligent Infrastructure (PII-FIRI)] under Grant 320019. The work of Matti Mäntysalo was supported by the Academy of Finland under Grant 288945 and Grant 292477. Recommended for publication by Associate Editor P. Xavier upon evaluation of reviewers' comments. (*Corresponding author: Mohammad H. Behfar.*)

Mohammad H. Behfar, Arttu Korhonen, Dung Nguyen, Timo Kurkela, and Markus Tuomikoski are with VTT Technical Research Centre of Finland, 90570 Oulu, Finland (e-mail: mohammadhossein.behfar@vtt.fi; arttu.korhonen@vtt.fi; dung.nguyen@vtt.fi; timo.kurkela@vtt.fi; markus.tuomikoski@vtt.fi).

Donato Di Vito and Matti Mäntysalo are with the Faculty of Information Technology and Communication Sciences, Tampere University, 33720 Tampere, Finland (e-mail: donato.divito@tuni.fi; matti.mantysalo@tuni.fi).

Belal Mostafa Amin is with the Circuit and System Research Unit, University of Oulu, 90570 Oulu, Finland (e-mail: belalmostafa30@gmail.com).

Color versions of one or more figures in this article are available at <https://doi.org/10.1109/TCPMT.2021.3082647>.

Digital Object Identifier 10.1109/TCPMT.2021.3082647

and stretchable substrates. Traditional wearable sensors utilize rigid electronics enclosed by hard covers, which can potentially fail to comply with dynamic deformations of the skin. The importance of user experience is profound in life-saving wearable medical sensors, where patient compliance to wear the sensors for prolonged time is essential. Therefore, improving the user experience requires redefinition of the concepts for wearable devices to become ultra-thin, lightweight, breathable skin patches that can comply with the deformations of the human body.

Several studies mainly focused on laboratory-scale development of novel flexible and stretchable sensors for biochemical sensing, physiological monitoring, and biomechanical strain measurement [1]–[7]. Those efforts successfully advanced in fabrication of stretchable sensing elements and components as sub-circuitry of a full system. Moreover, other studies demonstrated the application of printed electrodes on thermoplastic polyurethane (TPU) for electrocardiography (ECG) measurement [8], which can be connected to reusable wearable electronics with cloud-based analytic tools [9]. However, in the proposed hybrid system, the detachable electronics is connected to the TPU-based patch with a USB connector. As alternatives to that type of hybrid system, different implementations for fully integrated skin-mounted devices were introduced. Some research reported microfluidic-aided assembly of conventional electronic components on elastic materials to form stretchable epidermal electronics [10], [11]. In those works, the key concept was to develop a mechanically compliant system using microfluidic suspensions of interconnects between the rigid components. Other studies also reported fully integrated systems for physiological monitoring where the electronic components are mounted on ultra-thin copper layers laminated between layers of stretchable polymer [12], [13]. Although all the aforementioned developments excelled in the prototyping phase, feasibility of scalable fabrication of sensors and systems on soft and elastic substrate requires reconsideration of the development process and materials to achieve reduced complexity for high-throughput manufacturing. To that end, further efforts were made to develop roll-to-roll fabrication of flexible electrochemical sensors for sweat analysis [14], [15].

In this work, we present a fully integrated, all-in-one wireless stretchable ECG signal acquisition system based on soft and elastic substrate as shown in Fig. 1(a). The key development concepts for the proposed ECG device are: 1) high stretchability; 2) durability; and 3) compatibility with

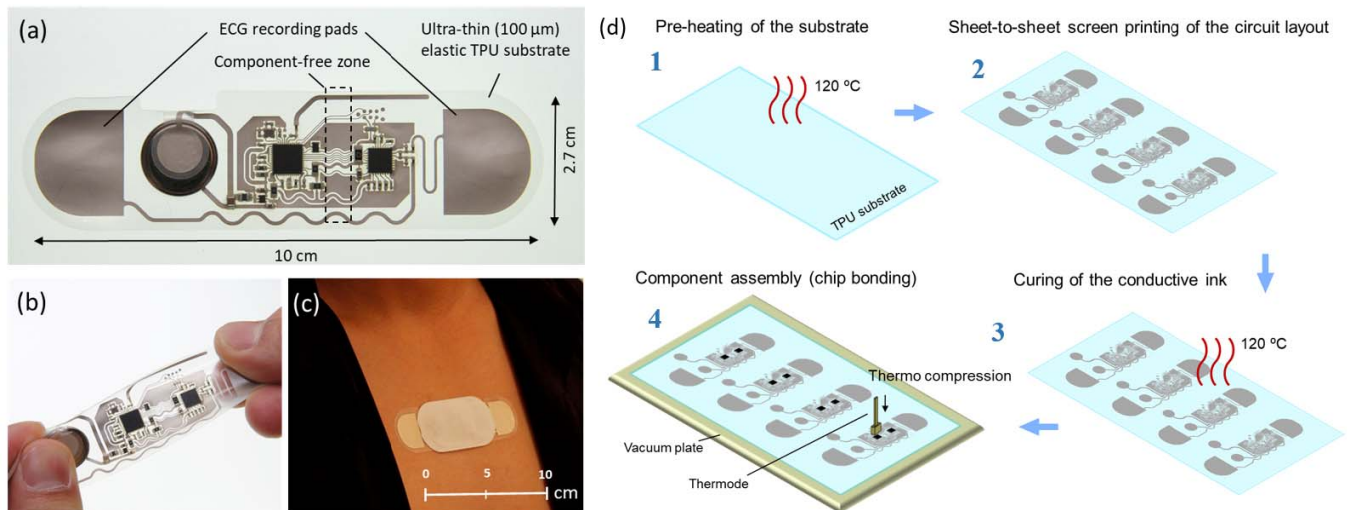


Fig. 1. (a) Fully integrated elastic ECG device. (b) Demonstration of stretchability of the soft device. (c) Conformity of the ultra-thin elastic patch when attached on chest. The electronics and battery are covered by additional TPU films (in white) on both the top and bottom layers. (d) S2S processing of the ECG circuit layout printing and chip bonding.

high-throughput manufacturing process. This study mainly focuses on sheet-to-sheet (S2S, also known as sheet-fed) processing of the stretchable device and its electromechanical performance over cyclic strain at 5% and 10% elongation. Despite that, the elastic devices in this work were fabricated using S2S automated printing and assembly machinery, all the development steps are truly roll-to-roll compatible. Combined experimental and *in silico* approaches were utilized to localize the failure points during cyclic strain. Finite element modeling (FEM) proved to be a useful technique to analyze and predict the mechanical deformations of surface-mounted components on simple stretchable devices [16], [17]. Particularly in this study, FE analyses were used in combination with the experimental electromechanical reliability tests to spot the potential failure points that are not easily accessible for visual inspection or electrical testing due to the supporting (encapsulation) layers.

II. SYSTEM DEVELOPMENT AND ASSEMBLY

A. Elastic ECG System Design

The ECG device comprises an ultralow-power, Bluetooth-enabled MCU (nRF52832, ARM Cortex-M4) and a dedicated single-channel ECG frontend (MAX30003). The system is driven by customized embedded software, enabling the device to operate in ultralow power mode with the battery life of up to 8 days (Lithium Coin, 60 mAh). The ECG device works with a companion mobile application to visualize the ECG data stream. Considering the conformity of the system to skin as the key feature of the wearable device, the layout and components distribution were engineered so that the ECG frontend and the MCU are separated by approximately 1 cm [see Fig. 1(a)]. This cleared area facilitates bending, stretching, and in general, deformation of the central part of the device without imposing excessive stress on the chips and passive components. Fig. 1(b) and (c) demonstrates stretchability of the soft elastic device and its conformity when attached to the skin, respectively. The connection between the MCU and

ECG frontend on the cleared area is the digital signal lines (serial communication bus), ensuring that the deformation of substrate in that area would not affect the signal quality.

B. Printing of the Circuit Layout and Chip Bonding

The circuit layout was screen-printed using stretchable conductive ink (EMS CI-1036) on an ultra-thin (100 μm), breathable and stretchable TPU (Covestro Plaiton U073) as illustrated in Fig. 1(d). The printing process was done by automatic offline sheet-fed screen printer (EKRA XH). Prior to the printing, the TPU film was pre-treated in an oven for 30 min at 120 $^{\circ}\text{C}$ in order to avoid any shrinkage during the printing process. The printed circuit layout was subsequently cured in an oven for 30 min at 120 $^{\circ}\text{C}$.

Component assembly was carried out using a sheet-fed and roll-to-roll bonding machine (Datacon 2200 EVO), which allows fast and versatile components bonding on silicon and polymer substrates. The machine was set to operate in stop-and-go mode so that assembly is performed on 200 mm (W) \times 300 mm (L) work area on halted foil. When the assembly is finished on the whole work area, the roll is transferred 300-mm forward and halted again for sequential assembly. Bonding of the components was performed using both isotropic and anisotropic conductive adhesives (ICA and ACA) as shown in Fig. 2(a). The passive components were bonded with ICA silver epoxy (Epotek H20E) and subsequently cured at 120 $^{\circ}\text{C}$ for 15 min. The main active components (MCU and ECG FE) were assembled using ACA (DELOMONOPOX AC245) followed by thermo-compression (weight: 350 g) at 230 $^{\circ}\text{C}$ for 70 ss. The temperature of vacuum plate underneath the circuitry was set to 65 $^{\circ}\text{C}$. After the bonding process, all the discrete components were encapsulated using UV-curable adhesive (DYMAX Ultra Light-Weld 9008) to improve endurance of the system during the stretching and deformations of the substrate [see Fig. 2(b)]. Moreover, encapsulation of the components enhances the stiffness of the surrounding region, which directs the strain concentration toward the stretchable part of the system [10], [18].

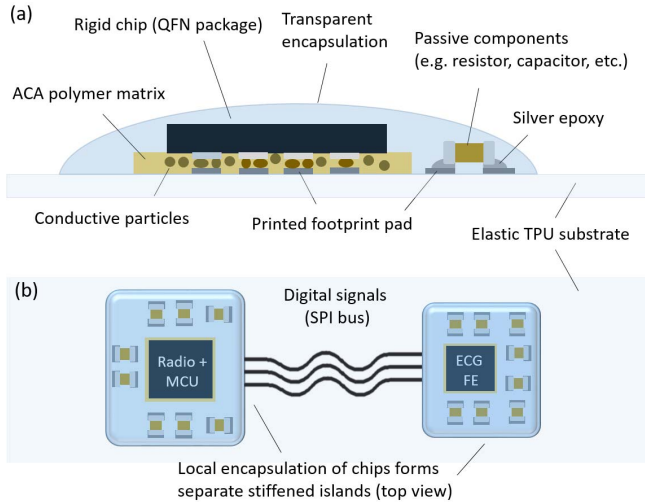


Fig. 2. (a) Graphical illustration of chip bonding and encapsulation of the active and passive components. (b) Isolated islands using transparent encapsulant.

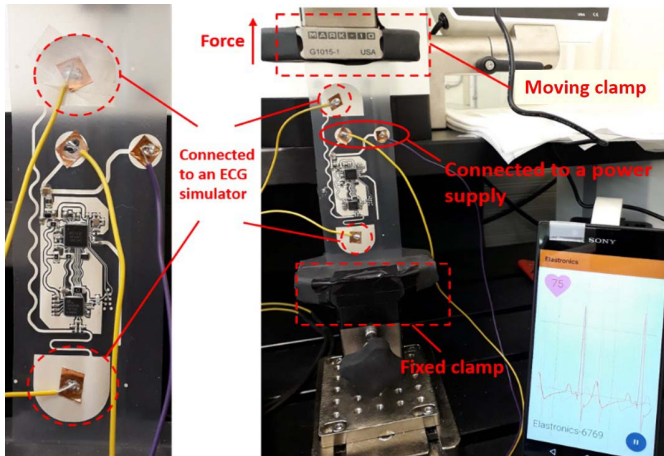


Fig. 3. Test setup for uniaxial cyclic strain at 5% and 10% elongation. The elastic device is connected to a power supply and ECG simulator while being stretched.

III. RESULTS AND DISCUSSION

A. Durability Test

A set of durability tests were conducted to evaluate the overall performance of the system under different cyclic uniaxial elongations. The ECG device consists of 31 components (4 active and 27 passive components). Practically, performance analysis of each single component is significantly difficult and requires complicated test setup. In order to ease the evaluation procedure, the overall performance of the system was defined as the ability of the system to be properly powered up, make a stable wireless connection to the mobile phone and stream valid ECG data, and accordingly, the system failure was defined as the malfunction of the device in any of the mentioned tasks. Two identical devices were used in the stretching test labeled as Devices 1 and 2. The test was performed using PC-controlled uniaxial tensile tester as shown in Fig. 3. The elongation of the elastic device ranged from 5% to 10% increase in length, that is, 6–12 mm when the distance between the fixed and moving clamps was set to 120 mm. The performance of the devices was monitored in

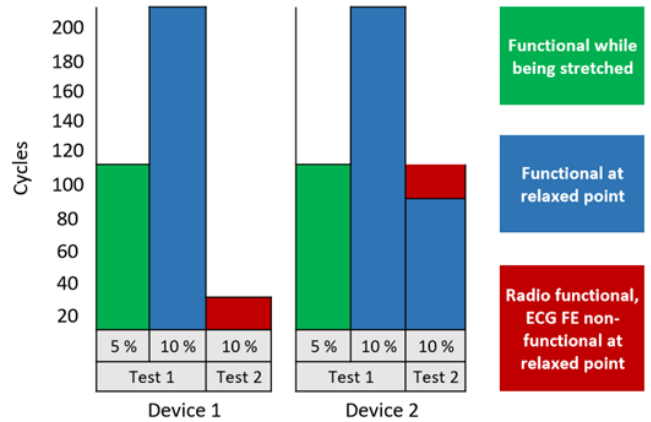


Fig. 4. Summary of uniaxial strain test of the elastic ECG devices at 5% and 10% elongation.

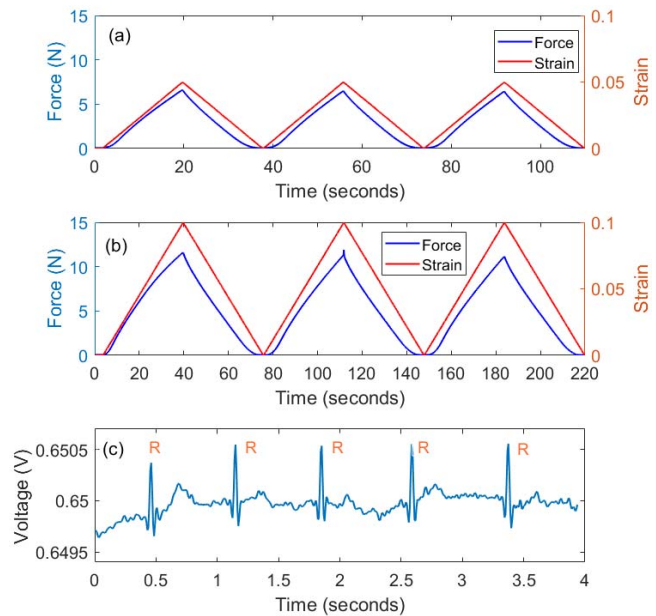


Fig. 5. (a) and (b) Applied forced and resultant strain at 5% and 10% elongation, respectively. (c) ECG data recorded with Device 2 after 400 cyclic strain from fingertips. The minor fluctuation on the baseline caused by the contact impedance between the finger and silver pads.

real time while being stretched using an ECG simulator and a mobile phone as the receiver. The durability study was structured into two tests per device, named as Test 1 and Test 2. For both devices, Test 2 was performed after Test 1 with a time gap of 10 days to allow possible recovery of the conductive lines and interconnections. In Test 1, the devices were tested under 5% and 10% stretch, whereas in Test 2, the devices were tested only under 10% stretch. In both tests, the stretching speed was set to 20 mm/min. A summary of the stretching test is given in Fig. 4. Both Devices 1 and 2 stayed functional while being stretched under cyclic 5% elongation. Our observation confirms that the system could maintain its overall performance as expected. At the peak of 10% elongation, both devices stopped collecting ECG data, while the BLE radio was still functional and the companion application could discover the device. However, when returned to the original length (after relaxation), the system operated normally and resumed data streaming. This can be explained by recovery

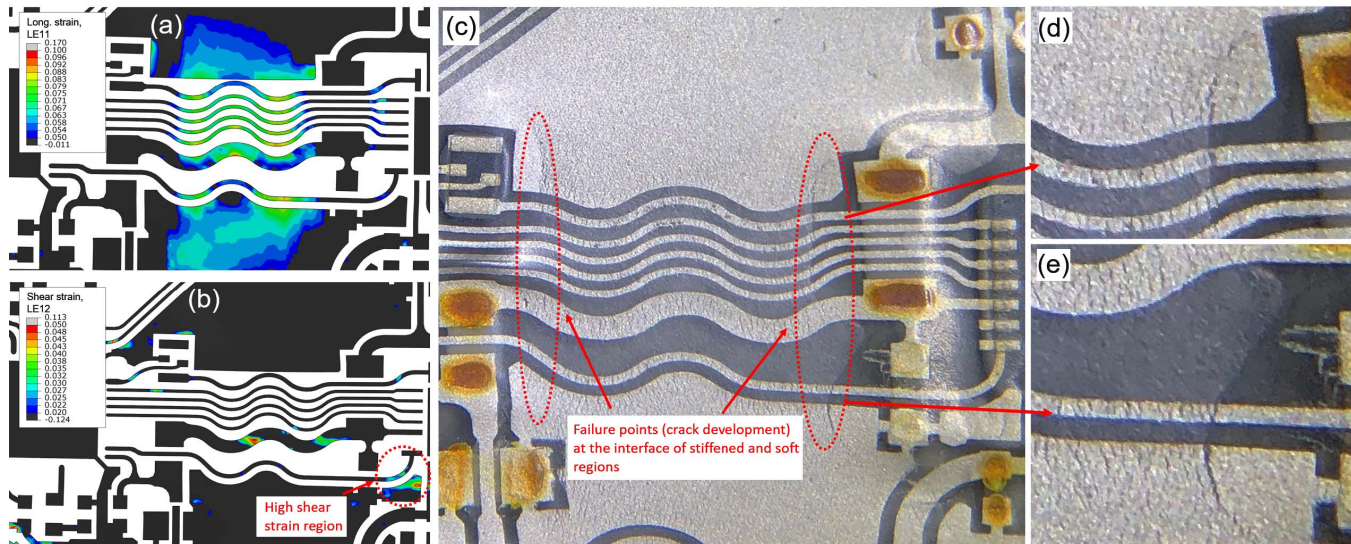


Fig. 6. (a) FE results showing the distribution of longitudinal deformations in the conductive layout. The contour plot focuses only on deformations higher than 5%, showing that the central part of the device undergoes higher deformation than its surroundings, due to the presence of the encapsulants on its sides. (b) FE results showing the shear strain during tensile deformation of the sample. It is possible to notice the high shear strain build-up in the curved part of the digital interrupt signal line (highlighted with a red dashed line), due to both the line shape and the presence of rigid components around that region. (c) Micrography of the back of the tested sample (mirrored) at 10% elongation. It is possible to distinguish the regions covered by the encapsulants, on the left and right side of the picture, and the central section, where a high crack density is visible on all the conductive lines, where electrical failure is estimated to occur. The crack orientation (vertical in this case) is reputed to be the main cause of electrical failure of the device. (d) and (e) Magnified detail of the formation of the crack in the rightmost region highlighted in Fig. 6(c).

of broken connections between the ECG frontend and the MCU at the relaxation point. In Test 2, the ECG frontend of Device 1 completely stopped responding to the MCU because of the broken interrupt signal line in early cycles of stretching. This issue was identified by software–hardware co-debugging. Device 2 showed the same behavior after 100 cycles in Test 2. Fig. 5(a) and (b) shows applied cyclic force and resultant strain at 5% and 10% elongation. The ECG signal recorded with Device 2 after almost 400 cycles (total in Tests 1 and 2) is shown in Fig. 5(c).

B. FEM Analyses and Failure Identification

The presence of the encapsulation layer, while improving the general performance of the system, makes it more complex to analyze the electromechanical status of the device after electrical failure. Thus, it is relied on a finite element model of the system to inspect the device under deformation and identifies possible failure locations under cyclic loading. For this reason, the FE model closely mimicked the structure of the sample under deformation and featured all the 43 rigid components present in the real device, together with the encapsulant, the substrate, and the conductive ink. The mechanical response chosen for the last two can be found in the previous works [16], [17], while the encapsulant was assumed to behave as a linear elastic material with a Young's modulus equal to 49 MPa. The bonding between the different components was assumed to be ideal without possible delamination and the loading conditions imitated the ones imposed by the tensile tester during 10% of tensile deformation imposed.

As can be seen from Fig. 6(a), the deformation around the MCU and the ECG frontend is mostly limited by the encapsulation layer. However, there is a reduction of the isolation

effect around the edges of the layer, where the deformation fields increase in magnitude due to the presence of rigid components bonded to the conductive tracks. In particular, the tensile deformation of the highlighted conductive lines reaches values over 5%, while the tensile deformation for the rest of the circuits is lower. Similar and higher values of deformation are also attained in the tracks connected to the ECG pads and to the battery; however, the line widths of those parts are more than five times the width of the digital lines mentioned. Among them, the digital interrupt signal line shows shear deformations higher than in the similarly sized digital conductive lines placed between the MCU and the ECG frontend, as can be seen in Fig. 6(b). This effect is due to the shape of the track and the components placed in its surroundings. Their presence, in fact, generates shear strain buildup throughout the substrate and the printed conductive layer due to their location and their bonding with the printed conductive layer. The FE results are in agreement with the cracking pattern found in the tested samples, as shown in Fig. 6(c), where it is possible to see that higher cracking density is achieved in the conductive track regions right next to the regions covered by the encapsulant, as was also noted and analyzed for simpler geometries in previous publications [16], [17]. While the encapsulant protects from surface cracking under tensile deformation, in fact, it also promotes the formation of stiffer regions, which in turn strongly influence the overall deformation behavior under tensile load. Thus, the creation of such “rigid islands” and their effect on the device deformation fields should be carefully considered when designing stretchable electronic devices, as their geometry and location with respect to sensitive electrical components and conductive tracks may have a strong impact on the overall performance of the device.

IV. CONCLUSION

Development of standalone stretchable devices requires careful consideration in system engineering, layout design, and material selection, in terms of both electrical and mechanical properties. Here in this work, a fully stretchable, wearable ECG system for mid/long-term ECG monitoring was developed and its behavior was analyzed in terms of electrical and mechanical response. The elastic system was fabricated on ultra-thin elastic and breathable substrate to provide comfortable wear experience. Moreover, the proposed processing is truly roll-to-roll compatible, allowing high throughput manufacturing, which is essential in translation of laboratory-scale prototyping to real-life applications. The TPU-based substrate facilitates post-processing and conversion of the device into soft and stretchable skin patches for direct contact with body. The durability of the devices was evaluated with 5% and 10% uniaxial cyclic strain. The strain test indicated the feasibility of durable hybrid integration of rigid components on stretchable materials without the need for interposer. Moreover, analysis of the deformation behavior of the device shed light on several important aspects that need to be taken into account when aiming to improve the electromechanical behavior of complex, printed stretchable electronic systems, such as the effect of encapsulant on the local stiffness and, consequently, on the deformation behavior under tensile loading.

The authors acknowledge that the performance of such a system should be tested under more complex conditions, including bi-axial strain and environmental tests (i.e., humidity and temperature) with higher number of samples. However, this study aimed at gaining a preliminary understanding on durability of such hybrid systems where considerable number of conventional passive and active components is assembled on a highly elastic substrate. In the same way, the complexity of predicting the deformed state through *in silico* methods increases due to the need to replicate the behavior of devices with complex electrical layout in detail. Nevertheless, the data acquired through FE analyses proved useful to accurately describe the failure behavior of the ECG device. Therefore, a deeper coupling of instruments for electrical and mechanical design seems to be necessary to further develop and improve the reliability of printed stretchable devices in a wide variety of loading conditions.

REFERENCES

- [1] H. Park *et al.*, "A skin-integrated transparent and stretchable strain sensor with interactive color-changing electrochromic displays," *Nanoscale*, vol. 9, no. 22, pp. 7631–7640, 2017, doi: [10.1039/C7NR02147J](https://doi.org/10.1039/C7NR02147J).
- [2] Y.-S. Huang, K.-Y. Chen, Y.-T. Cheng, C.-K. Lee, and H.-E. Tsai, "An inkjet-printed flexible non-enzymatic lactate sensor for clinical blood plasma test," *IEEE Electron Device Lett.*, vol. 41, no. 4, pp. 597–600, Apr. 2020, doi: [10.1109/LED.2020.2973343](https://doi.org/10.1109/LED.2020.2973343).
- [3] L. M. Ferrari, U. Ismailov, J.-M. Badier, F. Greco, and E. Ismailova, "Conducting polymer tattoo electrodes in clinical electro- and magneto-encephalography," *Npj Flexible Electron.*, vol. 4, no. 1, pp. 1–9, Mar. 2020, doi: [10.1038/s41528-020-0067-z](https://doi.org/10.1038/s41528-020-0067-z).
- [4] B. Nie, S. Xing, J. D. Brandt, and T. Pan, "Droplet-based interfacial capacitive sensing," *Lab Chip*, vol. 12, no. 6, pp. 1110–1118, Jul. 2012, doi: [10.1039/C2LC21168H](https://doi.org/10.1039/C2LC21168H).
- [5] H. Xu, J. Liu, J. Zhang, G. Zhou, N. Luo, and N. Zhao, "Flexible organic/inorganic hybrid near-infrared photoplethysmogram sensor for cardiovascular monitoring," *Adv. Mater.*, vol. 29, no. 31, Aug. 2017, Art. no. 1700975, doi: [10.1002/adma.201700975](https://doi.org/10.1002/adma.201700975).

- [6] S. M. Lee *et al.*, "Self-adhesive epidermal carbon nanotube electronics for tether-free long-term continuous recording of biosignals," *Sci. Rep.*, vol. 4, no. 1, pp. 1–9, Aug. 2014, doi: [10.1038/srep06074](https://doi.org/10.1038/srep06074).
- [7] Y. Zhang and T. H. Tao, "Skin-friendly electronics for acquiring human physiological signatures," *Adv. Mater.*, vol. 31, no. 49, Dec. 2019, Art. no. 1905767, doi: [10.1002/adma.201905767](https://doi.org/10.1002/adma.201905767).
- [8] T. Vuorinen *et al.*, "Validation of printed, skin-mounted multilead electrode for ECG measurements," *Adv. Mater. Technol.*, vol. 4, no. 9, Sep. 2019, Art. no. 1900246, doi: [10.1002/admt.201900246](https://doi.org/10.1002/admt.201900246).
- [9] T. Vuorinen *et al.*, "Unobtrusive, low-cost out-of-hospital, and in-hospital measurement and monitoring system," *Adv. Intell. Syst.*, vol. 3, no. 3, Mar. 2021, Art. no. 2000030, doi: [10.1002/aisy.202000030](https://doi.org/10.1002/aisy.202000030).
- [10] S. Xu *et al.*, "Soft microfluidic assemblies of sensors, circuits, and radios for the skin," *Science*, vol. 344, no. 6179, pp. 70–74, Apr. 2014, doi: [10.1126/science.1250169](https://doi.org/10.1126/science.1250169).
- [11] H. U. Chung *et al.*, "Binodal, wireless epidermal electronic systems with in-sensor analytics for neonatal intensive care," *Science*, vol. 363, no. 6430, Mar. 2019, Art. no. eaau0780, doi: [10.1126/science.aau0780](https://doi.org/10.1126/science.aau0780).
- [12] Y. Kim *et al.*, "All-in-one, wireless, stretchable hybrid electronics for smart, connected, and ambulatory physiological monitoring," *Adv. Sci.*, vol. 6, no. 17, Sep. 2019, Art. no. 1900939, doi: [10.1002/advs.201900939](https://doi.org/10.1002/advs.201900939).
- [13] H. Kim *et al.*, "Fully integrated, stretchable, wireless skin-conformal bioelectronics for continuous stress monitoring in daily life," *Adv. Sci.*, vol. 7, no. 15, Aug. 2020, Art. no. 2000810, doi: [10.1002/advs.202000810](https://doi.org/10.1002/advs.202000810).
- [14] M. Bariya *et al.*, "Roll-to-roll gravure printed electrochemical sensors for wearable and medical devices," *ACS Nano*, vol. 12, no. 7, pp. 6978–6987, Jul. 2018, doi: [10.1021/acs.nano.8b02505](https://doi.org/10.1021/acs.nano.8b02505).
- [15] H. Y. Y. Nyein *et al.*, "Regional and correlative sweat analysis using high-throughput microfluidic sensing patches toward decoding sweat," *Sci. Adv.*, vol. 5, no. 8, Aug. 2019, Art. no. eaaw9906, doi: [10.1126/sciadv.aaw9906](https://doi.org/10.1126/sciadv.aaw9906).
- [16] M. Mosallaei, D. Di Vito, B. Khorramdel, and M. Mäntyselä, "Improvements in the electromechanical properties of stretchable interconnects by locally tuning the stiffness," *Flexible Printed Electron.*, vol. 5, no. 1, Jan. 2020, Art. no. 015004, doi: [10.1088/2058-8585/ab68ae](https://doi.org/10.1088/2058-8585/ab68ae).
- [17] D. Di Vito, M. Mosallaei, B. Khorramdel, M. Kanerva, and M. Mäntyselä, "Mechanically driven strategies to improve electromechanical behaviour of printed stretchable electronic systems," *Sci. Rep.*, vol. 10, no. 1, pp. 1–11, Jul. 2020, doi: [10.1038/s41598-020-68871-w](https://doi.org/10.1038/s41598-020-68871-w).
- [18] N. Matsuhisa, X. Chen, Z. Bao, and T. Someya, "Materials and structural designs of stretchable conductors," *Chem. Soc. Rev.*, vol. 48, no. 11, pp. 2946–2966, Jun. 2019, doi: [10.1039/C8CS00814K](https://doi.org/10.1039/C8CS00814K).



Mohammad H. Behfar received the D.Sc. (Tech.) degree in biomedical sciences and engineering from the Tampere University of Technology (TUT), Tampere, Finland, in 2018.

From 2013 to 2014, he was with the Department of Advanced Technology Development, GE Healthcare, Helsinki, Finland, where he actively worked on hardware-software co-design of a medical-grade EEG recorder. During his time at TUT, his research focused on the development of a wireless platform for continuous monitoring of the intracranial pressure (ICP), from concept development to *in vivo* evaluation. As a part of his doctoral research program, he has worked as a Visiting Researcher with the Biodesign Laboratory, University of California at San Francisco, San Francisco, CA, USA. He is currently with the Flexible Electronics and Integration Research Team, VTT, Oulu, Finland. His research interests include printed stretchable electronics, smart skin patches, and epidermal electronics.



Donato Di Vito received the M.Sc. degree in materials engineering and the Ph.D. degree in industrial products and process engineering from the University of Naples Federico II, Naples, Italy, in 2013 and 2017, respectively.

He is currently a Post-Doctoral Researcher at Tampere University, Tampere, Finland. His current research interests include numerical modeling of mechanical behavior of highly deformable materials, with a focus on materials suitable for printed stretchable electronic applications.



Timo Kurkela received the B.Sc. degree in physics from the Faculty of Science, University of Oulu, Oulu, Finland, in 2013, and the M.Sc. degree in microsystems technology from the Faculty of Information Technology and Electrical Engineering, University of Oulu, in 2016.

He is currently with the Flexible Electronics and Integration Research Team, VTT, Oulu. His research interests include printed hybrid electronics design and system integration.

Arttu Korhonen, photograph and biography not available at the time of publication.



Dung (Daniel) Nguyen received the B.Sc. degree in computer engineering from the Ho Chi Minh City University of Technology, Ho Chi Minh City, Vietnam, in 2012, and the M.Sc. degree in computer science and engineering from the Faculty of Information Technology and Electrical Engineering, University of Oulu, Oulu, Finland, in 2019.

He is currently working as the Research Scientist of the Flexible Electronics and Integration Research Team, VTT, Oulu. His research interests include smart embedded software and electronics design.



Markus Tuomikoski received the M.Sc. degree in chemistry from the University of Oulu, Oulu, Finland, in 2001.

He was a Visiting Scholar with the Optical Sciences Center, The University of Arizona, Tucson, AZ, USA, in 2003. He is currently working as the Senior Scientist and the Project Manager of VTT Technical Research Center of Finland, Oulu. His particular research interest includes the development of hybrid integration technology for wearable sensor and communication applications.



Belal Mostafa Amin received the B.Sc. degree in communication and computer engineering from the Faculty of Engineering, Alexandria University, Alexandria, Egypt, in 2016, and the M.Sc. degree in RF engineering from the University of Oulu, Oulu, Finland, in 2020, where he is currently pursuing the Ph.D. degree with the Circuit and Systems Research Unit and his research work is focused on digital CMOS-based IC design.



Matti Mäntysalo (Member, IEEE) received the M.Sc. and D.Sc. (Tech.) degrees in electrical engineering from the Tampere University of Technology, Tampere, Finland, in 2004 and 2008, respectively.

From 2011 to 2012, he was the Visiting Scientist of the iPack Vinn Excellence Center, School of Information and Communication Technology, KTH Royal Institute of Technology, Stockholm, Sweden. He is currently a Professor of electronics at Tampere University, Tampere. He has authored more than 100 international journal articles and conference papers.

His current research interests include printed electronics materials, fabrication processes, stretchable electronics, and especially the integration of printed electronics with silicon-based technology (hybrid systems).

Dr. Mäntysalo was a recipient of the Academy Research Fellow Grant (2015–2020) from the Academy of Finland. He has served on the IEEE TRANSACTIONS ON COMPONENTS, PACKAGING AND MANUFACTURING TECHNOLOGY (CPMT), the IEC TC119 Printed Electronics Standardization, and the Organic Electronics Association.